Preparation of matrix-matched standards for the analysis of teeth via laser ablation-inductively coupled plasma-mass spectrometry

Mika T. Westerhausen[a], Martin Bernard[a], Gina Choi[a], Christine Jeffries-Stokes[b], Rohana Chandrajith[c], Richard Banati[d,e], David P. Bishop[a]

[a]*Hyphenated Mass Spectrometry Laboratory (HyMaS), School of Mathematical and Physical Sciences, Faculty of Science, University of Technology Sydney, P.O. Box 123, Broadway, NSW 2007, Australia.*

[b]*The Rural Clinical School of Western Australia • Kalgoorlie WA 6433 Australia*

[c]*Department of Geology, Faculty of Science, University of Peradeniya, Peradeniya, Sri Lanka*

[d]*Australian Nuclear Science and Technology Organisation, New Illawarra Rd, Lucas Heights NSW 2234*

[e]*University of Sydney, Faculty of Medicine and Health, 94 Mallett St, Camperdown NSW 2050*

Abstract

Mineralised tissue such as teeth can serve as a retrospective, chronological bioindicator of past exposure to toxic metals. Laser ablation-inductively coupled plasma-mass spectrometry (LA-ICP-MS) can be used to determine the presence and spatial distribution of toxic metals in teeth, giving a record of when an exposure occurred. Concentrations of these metals is often determined by a one-point calibration against NIST glass using an equation that requires an internal standard factor that accounts for differences in ablation behaviour between the glass and the tooth. However, an ideal external calibration would contain multiple matrix-matched standards to obtain a calibration curve. Here, we investigated optimal procedures for preparing synthetic hydroxyapatite (HA) doped with elements of interest as a calibration material. The materials were examined for homogeneity of metal incorporation, matrix-matched ablation characteristics, linearity, and limits of detection. A homogenised and pelleted HA was the most suitable material, providing improved ablation characteristics over previous HA materials and NIST glass for the analysis of teeth. An ablation yield of 1.1 showed its suitability to analyse teeth, the metals were homogeneously incorporated, and it produced excellent linearity with limits of detection ranging from 0.1-2 $\mu g\ kg^{-1}$ for magnesium, aluminium, nickel, copper, zinc, cadmium, barium and lead. A juvenile incisor from a remote indigenous community in Australia and an adult molar from Sri Lanka were assessed for heavy metal exposure. The molar showed evidence of exposure to cadmium and lead.

The synthetic HA material was straightforward to prepare, and will improve confidence in the analysis of teeth and other biomineralised material when assessing heavy metal exposure.

Introduction

Laser ablation-inductively coupled plasma-mass spectrometry (LA-ICP-MS) is a solid sampling technique that uses a focussed laser beam to aerosolise material from the sample surface. The material is then transported to the plasma by a carrier gas where it is ionised and introduced into the mass spectrometer, which selectively detects ions at a given mass-to-charge ratio. Its unique solid sampling approach can provided localised information via spot analysis or provide spatial information by reconstructing images based on line ablation across a sample, and is advantageous due to its low limits of detection for the majority of elements and minimal sample destruction[1]. LA-ICP-MS is an established technique for the elemental analysis of geological and metallurgical samples, and the softer biological tissues where calibration materials are well-characterised[2,3]. The technique has further been applied to calcified tissues to analyse environmental changes or pollutant accumulation within the incremental growth layers of biomaterials such as scales[4], shells[5], otoliths[6], and tree xylem[7]. The analysis of elemental composition of teeth is of interest as it may create temporal profiles of metal exposure during early development where variations over days or months need to be studied, making sensitivity of analysis a priority[8–11]. Quantification of these harder biological tissues is often achieved via calibration materials that are not fit for purpose.

The biomineral component of teeth and bones, hydroxyapatite ($Ca_{10}(PO_4)_6(OH)_2$), is formed within the body under direct physiological control, and hence reflects the trace metals load and state of metabolism[12]. Teeth continues this process throughout an individual's lifespan, offering a chronological record of heavy metal contaminants in both food and water[9,10,13,14]. Previously, quantification of elements in teeth have used NIST SRM 610 or 612 glass reference materials[13], bone meal (SRM 1486) and bone ash (SRM 1400)[15]. Use of NIST SRM glass relies upon a quantification method originally developed for the analysis of other glass materials, however it has been implemented for the analysis of highly mineralised tissues

such as otoliths and teeth[14,16]. The method first developed by Longerich *et al.*[17] relies upon the use of a "naturally occurring" internal standard in order to produce a robust calibration, allowing for correction of sensitivity drift, matrix effects and differences in the amount of sample ablated relative to the calibration material. The concentration is obtained by dividing the response of an analyte over the normalised sensitivity, which is defined as;

$$S = \frac{R_{AN_{CAL}}}{C_{AN_{CAL}}}\left(\frac{R_{IS_{SAM}}}{R_{IS_{CAL}}}\frac{C_{IS_{CAL}}}{C_{IS_{SAM}}}\right) \quad (1)$$

Where S is the normalised sensitivity, $R_{AN_{CAL}}$is the count rate of the analyte in the calibration material, $C_{AN_{CAL}}$is the concentration of the analyte in the calibration material, $R_{IS_{SAM}}$ is the counts of the internal standard in the sample, $R_{IS_{CAL}}$ is the counts of the internal standard in the calibration material, $C_{IS_{CAL}}$ is the concentration of the internal standard in the calibration material and $C_{IS_{SAM}}$ is the concentration of the internal standard in the sample.

In this equation, the sensitivity is normalised to the mass of the sample ablated via the response and concentration of the internal standard in the sample and the calibrant. If the ablated mass, or ablation yield, of the sample and the calibrant were the same, the normalisation factor would equal 1. The concentration of the internal standard can be determined using another quantitative technique or from the known elemental stoichiometry when crystalline materials are analysed. This equation is widely used for the LA-ICP-MS analysis of hard materials without fully matrix-matched standards, however the technique requires frequent recalibration to correct for mass-dependent drift. This resulted in this equation being described as semi-quantitative, and in need of validation for the quantitative elemental analysis of calcified tissues such as teeth[18].

Matrix-matched synthetic hydroxyapatite materials doped with analyte metals were developed to improve quantification of calcified tissues[15,19–21]. However, issues arose from being unable to obtain matched ablation behaviour between the calibration material and the sample[15], with neither ablation yield or normalised sensitivity reported. Previous hydroxyapatite standards suffer from elemental inhomogeneity with relative standard deviation (RSD) up to 32% due to grain size and poor uptake into the crystal

lattice[22,23]. Sintered hydroxyapatite was proposed as a solution to this inhomogeneity[24], but has known issues with elements such as copper melting between crystal grains resulting in high %RSD[25]. Here we describe the preparation and validation of homogenous synthetic hydroxyapatite standards for the analysis of teeth that include elements known to be affected by sintering. Three preparation methods were examined to see which best incorporated the analyte elements into its material and matched the ablation behaviour of teeth. The optimised calibration material was then applied to determine the spatial quantification of elements in a primary incisor and a molar tooth.

Experimental

Tooth mounting & Sectioning

Two teeth samples were analysed, a juvenile primary incisor collected from a remote community in Western Australia, and an adult deciduous third molar collected from Sri Lanka. Prior to analysis, the teeth were washed in an ultrasonic bath in a solution of 2% hydrogen peroxide and ultrapure water. The teeth were subsequently rinsed with ultrapure water to remove impurities. The teeth were then mounted in epoxy resin and sectioned into 1 mm sections in plane passing the root tip and crown cusp on a low-speed rotary saw equipped with a 0.3 mm scintillated diamond saw blade. The epoxy resin was then removed from the tooth sections using chloroform due to poor attachment between resin and tooth, the sections were subsequently rinsed repeatedly with ultrapure ethanol followed by ultrapure water.

Chemicals & Reagents

The ultrapure water was obtained from a Sartorius Arium Pro Vf (Göttingen, Germany). High purity element standards and SEASTAR Baseline ultrapure nitric acid (HNO_3), hydrochloric acid (HCl) and hydrogen peroxide (H_2O_2), were purchased from Choice Analytical (Thornleigh, NSW, Australia).

Synthesis of doped hydroxyapatite calibration materials

Three sets of five co-precipitated hydroxyapatite (HA) standards containing magnesium (Mg), aluminium (Al), nickel (Ni), copper (Cu), zinc (Zn), cadmium (Cd), barium (Ba), and lead (Pb), and corresponding blank HA, were prepared. Hydroxyapatite was precipitated from calcium nitrate tetrahydrate

($Ca(NO_3)_2 \cdot 4H_2O$, Merck, Darmstadt, Germany) and ammonium dihydrogen phosphate ($NH_4H_2PO_4$, Merck, Darmstadt, Germany). 0.25 mol L^{-1} $Ca(NO_3)_2 \cdot 4H_2O$ and 0.15 mol L^{-1} $NH_4H_2PO_4$ solutions were prepared in ultrapure water, and the pH of the $NH_4H_2PO_4$ solution was adjusted to 10 by addition of ammonium hydroxide (NH_4OH, 25 %, Merck, Darmstadt, Germany). 25 mL of the $NH_4H_2PO_4$ solution was added drop-wise to 25 mL of the $Ca(NO_3)_2 \cdot 4H_2O$ solution. To dope the hydroxyapatite standards with trace elements, the $Ca(NO_3)_2 \cdot 4H_2O$ was spiked with 50, 100, 250, 500, and 1000 µL of multi-element standard solution calibration solution (10 mg L^{-1} Multi-element calibration standard-2A, Agilent Technologies, Santa Clara, California, United States) prior to the addition of $NH_4H_2PO_4$. The concentration of each element in the spiked solution was adjusted to achieve a suitable final concentration in the doped hydroxyapatite standard for external calibration of teeth samples by LA-ICP-MS. Each set of calibration standards were centrifuged at 3000 rpm for 15 min, the supernatant was then decanted off, and the precipitate dried in an oven at 60ºC for 24 hours. One set of the resulting amorphous crystal HA calibration standards were prepared for analysis by LA-ICP-MS by sanding a single crystal into a pellet and mounting onto a glass slide with double sided tape. The second set of HA standards were manually homogenised into a HA powder in a ceramic mortar until the particle size no longer visually reduces from grinding (roughly 10 minutes) in a similar manner to the method of Ulens *et al*. for analysing marble crusts[26]. Approximately 100 mg of the HA powder was pressed into a 10 mm diameter disc at a pressure of 6.8 tons. The third set of HA standards were created by pelleting the HA powder and sintering at 1000 ºC for 3 hours prior to mounting on a glass slide with double sided tape.

Characterisation of the elemental content in the HA standards

The concentrations of the analytes in the HA standards was determined by acid digestion and solution ICP-MS. For determination of the analyte concentrations approximately 10 mg of each pellet was transferred to polypropylene tubes (1.5 mL; Eppendorf Macquarie Park NSW, Australia) and weighed (three replicates). Digestion was achieved by shaking the portion of HA standard in 200 µL of 20% HNO_3 and 15% HCl, followed by dilution to 1.5 mL. All HA standards were analysed on an Agilent 8900 ICP-

MS (Agilent Technologies, Mulgrave, Australia) in single quadrupole mode equipped with a Micromist nebuliser and Scott type double pass spray chamber cooled to 2ºC for sample introduction. A 100 µg L^{-1} rhodium solution in 1% HNO_3 was used as an internal standard and introduced into the analyte flow via a T connector post-pump, and platinum sampling and skimmer cones were used. The 8900 ICP-MS was controlled by Agilent Technologies ICP-MS Masshunter software on a Hewlett-Packard (Hewlett-Packard Palo Alto, CA) desktop computer.

LA-ICP-MS Imaging

LA-ICP-MS was performed using an Elemental Scientific Lasers NWR193 ArF excimer laser (Kennelec Scientific, Mitcham VIC, Australia) hyphenated to an Agilent 8900 ICP-MS (Agilent Technologies, Mulgrave, Australia). Typical LA-ICP-MS parameters are shown in Table 1. NIST 612 Trace element Glass CRM was ablated to determine optimal ICP-MS parameters to maximise sensitivity and ensure minimal oxide formation (ThO/Th<0.3%). Laser ablation was optimised from 1% power up to the minimum threshold (10% power) of tooth ablation to minimise thermalisation and other high energy ablation effects.

All LA-ICP-MS experiments were performed using raster line sampling with scan speeds and ICP-MS dwell times set according to the optimal parameters identified by Lear *et al.*[27]. The images were reconstructed using Pew[2] visualisation software[28], and either quantified in the software or by exporting the image as a .csv for single point calibration with NIST 612 glass in Microsoft Excel. Image data calibrated in Excel was then exported as a .csv for processing in the FIJI ImageJ software package.

Table 1. Typical LA-ICP-MS parameters used for analysis

New Wave Excimer 193		Agilent 8900x	
Laser Fluence	0.4 mJ cm^{-2}	<u>Sample Introduction</u>	
Laser Power	10%	RF Power (W)	1500
Spot Size	50 µm	Carrier gas flow rate (L min^{-1})	1.2
Scan Speed	100 µm s^{-1}	Makeup gas flow rate (L min^{-1})	0.0

Frequency	80 Hz	Sample depth, mm	5.0
		Ion lenses	
		Extracts 1, 2 (V)	-12.0, -160.0
		Mega bias, lens (V)	-110, 3.4
		Cell entrance, exit (V)	-50.0, -2.0
		Octopole parameters	
		Octopole RF (V)	180
		Octopole bias (V)	-14.0

The two sections of deciduous teeth samples (one canine and one molar)were analysed by LA-ICP-MS under the same conditions as the reference materials and the NIST 612 glass for quantitative analysis. Elemental images were obtained using all calibration curves established from ablating the three HA matrix-matched standards prepared here, and using the single point calibration from comparison with NIST 612 glass according to the equation described by Longerich *et al.*[17].

Analytical performance of the HA calibration standards

The analytical performance of the three HA calibration materials were compared against each other and NIST 612 using the Longerich equation for all analytes. Ca was also monitored to determine the ablation yield ratio, r, of the standards compared to the whole of each tooth sample (to compensate for the variability of ablation over different parts of a tooth[29]) using the internal standard factor accounting for the mass of material ablated taken from the Longerich equation.

$$r = \frac{R_{IS_{SAM}}}{R_{IS_{CAL}}} \frac{C_{IS_{CAL}}}{C_{IS_{SAM}}} \quad (2)$$

The most suitable matrix-matched calibration material was identified as the material with an ablation yield ratio closest to 1. The limits of detection (LOD), limits of quantification (LOQ), and the linearity (r^2) value were also considered. Calibration curves were weighted using a least squares regression to remove bias caused by the high concentration standards.

LODs were determined from the weighted calibration curves for each analyte using the formula;

$$LOD = \frac{(y_0 + 3.3s_{xy})}{m} \quad (3)$$

Where y_0 is the weighted cps of the blank HA, s_{xy} is the standard deviation of the LA-ICP-MS measurement of the corresponding analyte signal of the HA blank, and m is the slope of the calibration.

Optical Microscopy

A Nikon Eclipse Ni microscope equipped with 5x, 10x, 20x, and 50x objectives, 10x eyepiece, and a Nikon DS-Fi2 camera was used for brightfield microscopy. The 5x objective was used to raster capture entire teeth and Nikon NIS Elements Control software was used to stitch the images together.

Scanning Electron Microscopy

Prior to scanning electron microscopy (SEM), the samples were sputtered with 20nm Gold/Palladium using a Leica EM ACE600 High Vacuum Coater. Micrographs of HA standards and molar tooth were performed using a Thermo Fisher Scientific Helios G4 Dual Beam microscope with a beam energy of 10.0 keV and a beam current of 0.2 nA.

Results and discussion

Characterisation of the hydroxyapatite calibration standards

The three HA materials prepared were characterised to determine their suitability as calibration standards for the analysis of teeth. The factors assessed for suitability included the degree of co-precipitation of each analyte metal, the homogeneity, the analytical performance, and the matrix matching through comparison of the ablation yield. Finally, each method was compared against the current single-point calibration method using NIST glass and the Longerich equation.

The amorphous HA crystal was the simplest to prepare and was the basis of the pelletised and sintered HA materials. Solution ICP-MS of the digested amorphous HA crystal standards showed that the analyte metals successfully co-precipitated into the material, however the high standard deviations across the three digests suggest that they were not homogenously distributed (see Supplementary Table 1). The

concentrations of metals obtained from within the structure were also higher than that initially spiked into the reaction mixture. This may be a result of unincorporated metals drying on the matrix, which, given standard "coffee-stain" drying patterns, would explain the high standard deviations. This preconcentration did not correlate with a previous study that reported optimal conditions for HA precipitation did not result in complete incorporation of the analytes into the material[1]. However, these studies used higher initial concentrations for precipitation. This suggests there is a limit to the level of substitution for each analyte metal depending on their individual and group properties.

LA-ICP-MS analysis of the amorphous HA crystal standards confirmed that the analytes were not homogenously distributed. Ablation of 4 lines of 2 mm length in the HA crystal calibration standards showed %RSDs ranging from 21-38% (see Supplementary Table 2 and Supplementary Figure 2). This inhomogeneity led to the removal of the two lowest concentration calibration levels due to the poor signal observed. This impacted the linearity of the calibration curves, with r values ranging from 0.96-1.00 across the four calibration levels (Supplementary Table 3), and the resulting LODs ranged from 0.7-4 μg kg^{-1} (Supplementary Table 4). Furthermore, the average ablation yield ratio was determined to be 2.56 (Table 2). As a comparison against standard methods, the ratio was determined for NIST glass, and a value of 81.6 was obtained. The high value is likely due to NIST glass being a polycrystalline blue transparent glass, whereas the various HA standards are all opaque white porous material, which means the laser ablation absorbance is different for wavelength, structure, and density of the two standards[30]. These results show that the calibration standards prepared from synthetic HA improve on current methods, and that the amorphous HA crystals ablate similarly to teeth, however it is still not optimal as it was inhomogeneous compared to the NIST glass.

The second HA calibration material was prepared through homogenisation of the amorphous HA crystal into a powder, followed by pelleting. Solution ICP-MS showed that the analyte metals were incorporated into the HA, and that homogenisation mitigated the variability of the crystallisation process. The lowest calibration point for Cu was below the LOD and was removed from the calibration curve.

Ablation of the pelleted HA powder confirmed the advantages of homogenisation. Ablation of 4 lines of

2mm in calibration standard showed %RSDs from 6-14% across all the elements investigated. This resulted in improved linearity with all elements apart from Cu (0.98), which is known to have poor co-precipitation in synthetic HA[31], exhibiting r greater than 0.99, with LODs ranging from 0.1-2 μg kg^{-1}. The average ablation ratio of this material was 1.09, demonstrating that this material ablated in a similar manner to teeth and is therefore suitable for calibration standards.

The final calibration material examined involved sintering the pelleted HA powder. Sintering was expected to result in improved ablation characteristics based upon prior results by Martinez et al for external standards prepared for the analysis of teeth by laser induced breakdown spectroscopy[1]. Solution analysis showed a large reduction in analyte concentrations in the standards, along with a concomitant increase in concentration in the blank.

Table 2. The ablation yield (*S*) determined for each calibration material

	Amorphous Crystal HA	Pelletised Powder HA	Sintered HA	NIST612
Blank	2.18	0.98	9.0	
Level 1	2.01	1.22	11.0	81.6
Level 2	2.77	1.12	11.6	
Level 3	2.49	0.99	15.8	
Level 4	3.06	1.17	21.2	
Level 5	2.84	1.08	12.3	
Average	2.56	1.09	13.5	81.6
%RSD	15.9	8.8	32.7	

Ablation of the sintered calibration material identified that the sintering process also reduced the homogeneity achieved through the pelleting process, with %RSDs ranging from 13-53%. The elements with the higher %RSDs, Zn, Cu, and Al, have melting temperatures lower than 1000°C, suggesting that the elements were heterogeneously redistributed via melting due to the high temperatures used during

sintering. Additionally, Zn was previously observed to migrate to voids within a HA matrix during sintering[32]. The high mobility of analytes from the calibration standards impacted the analytical figures, with the linearity ranging from 0.54-0.99, and LODs from 1-80 μg kg^{-1}. This elemental mobility in sintered HA decreases the feasibility of the preparation of multi-element multi-point standards with a globally suitable range and accuracy. The sintered HA standards also produced the worst average ablation ratio of the prepared HA materials (13.5), further demonstrating its unsuitability as a matrix-matched calibration material.

SEM was used for further characterisation of the calibration materials. SEM micrographs (Supplementary Figures 4-6) of each calibration material and a molar tooth show mixed morphology. HA crystal had the most similar porosity to the molar tooth dentin but had a larger particle size, pelletised HA and the molar tooth dentin had comparable porosity and particle sizes with a range from 1-5μm, and the sintered HA exhibited the least similar morphology to the molar tooth dentin.

The three calibration materials were further examined by analysing a tooth sample and comparing values against the single point calibration using NIST glass, with Figure 1 showing the results for Pb. The pelleted powder, with the similar ablation characteristics, produced the lowest values, followed by the amorphous HA crystal, the NIST glass, and the sintered glass. The values produced by the sintered glass are an estimate only due to the large analyte loss during the sintering process, and the high variability in the obtained signal. Representative line scans and calibration curves of each calibration material for Pb (Supplementary Figure 2 and 3), further demonstrates the differences in homogeneity described above and in Table 2.

These results show that the pelleted synthetic HA standards were the most appropriate material for preparing calibration standards in the analysis of teeth. Analytes were homogenously distributed, and exhibited excellent linearity and LODs. With an ablation yield ratio of 1 the pelleted HA standard ablated in an identical manner to the teeth, and to the author's knowledge is the closest matched artificial matrix prepared to date. In comparison NIST 612, the benchmark standard reference material for quantifying tooth samples, has an ablation yield 80 times higher than the pelleted HA standards. The LOD values

obtained here for Cd, and Pb were respectively 7 and 36 times lower than those obtained previously using HA standards and LA-ICP-MS analysis (Cd=0.2, Pb=0.1 µg kg^{-1} compared to Cd=1.4, Pb=3.6 µg kg^{-1})[19], 100 and 900 times lower than Al and Ba quantification using NIST standards on a LA-ICP-tof-MS (Al=0.2, Ba=0.1 µg kg^{-1} compared to Al=20, Ba=90 µg kg^{-1})[33], and 260 times lower for Ni than results obtained on sintered HA standards and laser induced breakdown spectroscopy (Ni=0.3 µg kg^{-1} compared to Ni=78 µg kg^{-1})[1]. Figure 1 highlights that higher ablation yields in the NIST standards may overestimate the concentrations obtained.

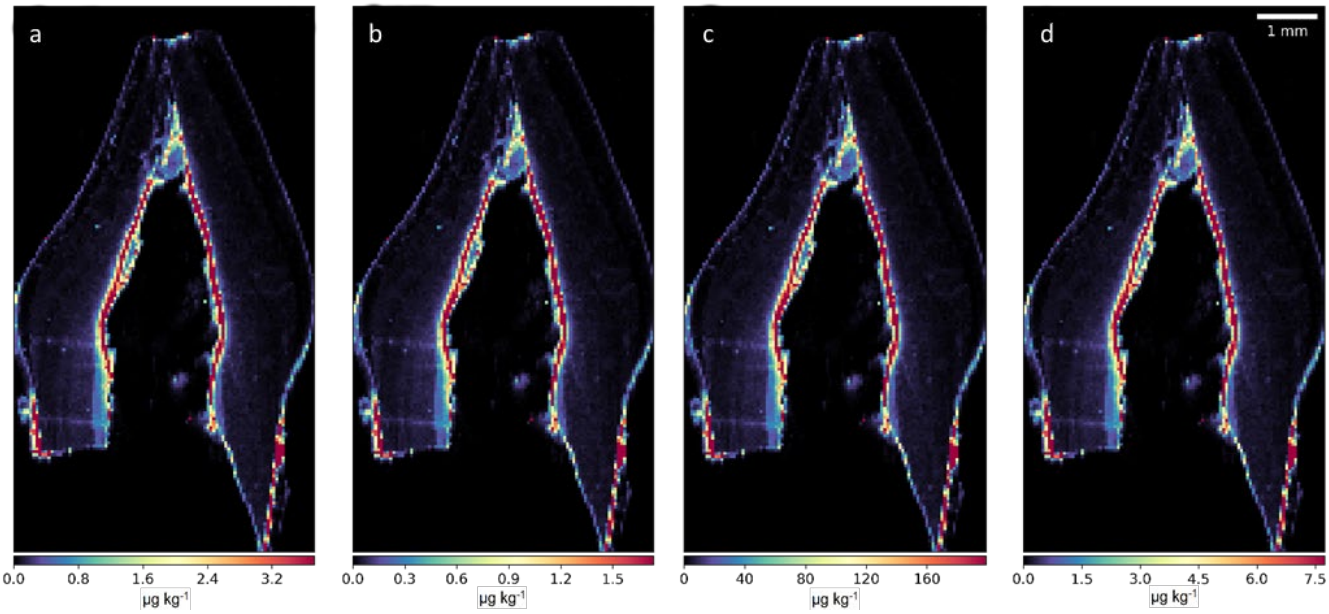

Figure 1. Comparison of Pb images obtained with the 4 calibration methods: a) amorphous HA powder, b) pelletised HA powder, c) sintered HA and, d) NIST612 Glass

Barium, calcium, lithium and strontium are the most commonly analysed elements in teeth via LA-ICP-MS due to their levels being ratiometrically or quantitatively correlated to nutritional and developmental stages during the life cycle[34]. Additionally, manganese has been investigated as an element of concern with early exposure suspected to affect neurodevelopment[35]. Most investigations of these elements in teeth use either NIST 612 or NIST 1486 bone meal certified standard materials for quantification[13,34–36], and NIST 610 or NIST 614 to assess signal drift[37]. Single point calibration standards have comparatively worse limits of detection compared to the multi-point calibration standards we have developed. Using naturally sourced material comes with the additional sensitivity issue of endogenous elemental

composition which increases the background signal, possible above the level of a biomarker element in a disease model which can be controlled for in synthetic materials such as the HA. The one noted exception being the use of a seal tooth and a clam shell with modern seawater values of 87Sr/86Sr to assess Australopithecus africanus teeth[37]. Other HA calibration standards suffered from elemental mobility during synthesis[32], required calcium normalisation[38], or contained elemental incorporation limits[39], none of which were observed using the method described here, culminating in increased accuracy of matrix-matched standards that contain more elements and calibration points than previously published for the quantification of teeth.

Analysis of metal distribution in teeth

The determination of elements in the Sri Lankan adult deciduous third molar is presented in Figure 2. Even though dentin thickness differs between sexes[40], deciduous and permanent teeth[41], and types of teeth[42], the mineral content[43] and dentin density[44] are similar enough to be considered the same when sampled using laser ablation[45]. Therefore, the analysis of 2 different types of deciduous teeth is suitable for matrix matching assessment. The intensities for Al, Cr Cu, Cd, Ba and Pb across the entire tooth section were quantified using the optimal external calibration material prepared via the co-precipitation of analyte metals in pelletised HA powder. The magnitude of the calibrated elemental intensities follow the pattern of Cu>Ba>Al>Cd>Pb>Ni>Cr. This order is contrary to the average total elemental concentration in dental tissue found in a tooth from Mexico[10], highlighting that the location impacts the metal uptake into teeth. Higher concentrations of Cu, Cd, and Pb were centralised in the dentin-pulp cavity as previously established[10,13,46]. This is a result of both the slow excretion of cadmium[47] combined with the exchange of secondary dentin with blood and organic matter that occurs in the pulp cavity, that Pb circulates in the blood and is not excreted by either dialysis treatments or the kidneys[48], and that heavy metals can be in a state of continual mineral exchange in the pulp cavity[49]. The juvenile incisor, similar to the molar, showed Pb and Cd in the pulp cavity (see Figure 1 and Supplementary Figure 1).

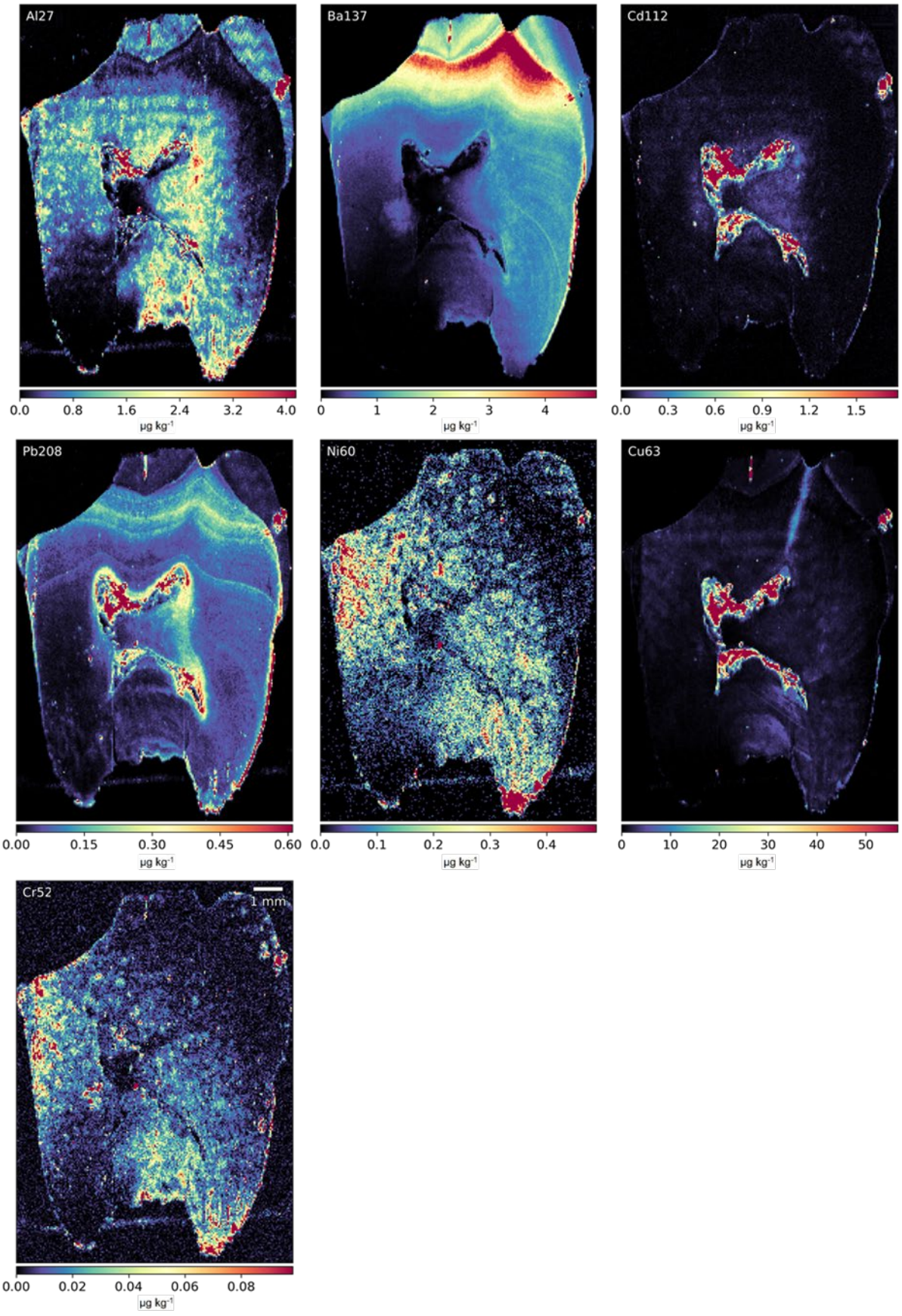

Figure 2. Quantified element distribution in the deciduous third molar using the pelletised HA standards.

The calibrated intensities for Pb in the Sri Lankan deciduous third molar show intense bands that correlate to the incremental growth markings that can be observed in the optical micrograph (Figure 3), confirming that LA-ICP-MS analysis can be used to establish a time-based record of exposure for lead due to the manner in which it is deposited into tooth dentin during calcification. Once a rate of deposition of the daily growth layers in terms of striations per day is determined, a time-based profile of the record of Pb exposure can be created by overlaying optical micrographs with the elemental distribution profile of lead (see Figure 3). As previously established[50], elevated levels of lead in pulp-dentin and across tooth dentin correlate to elevated environmental exposure.

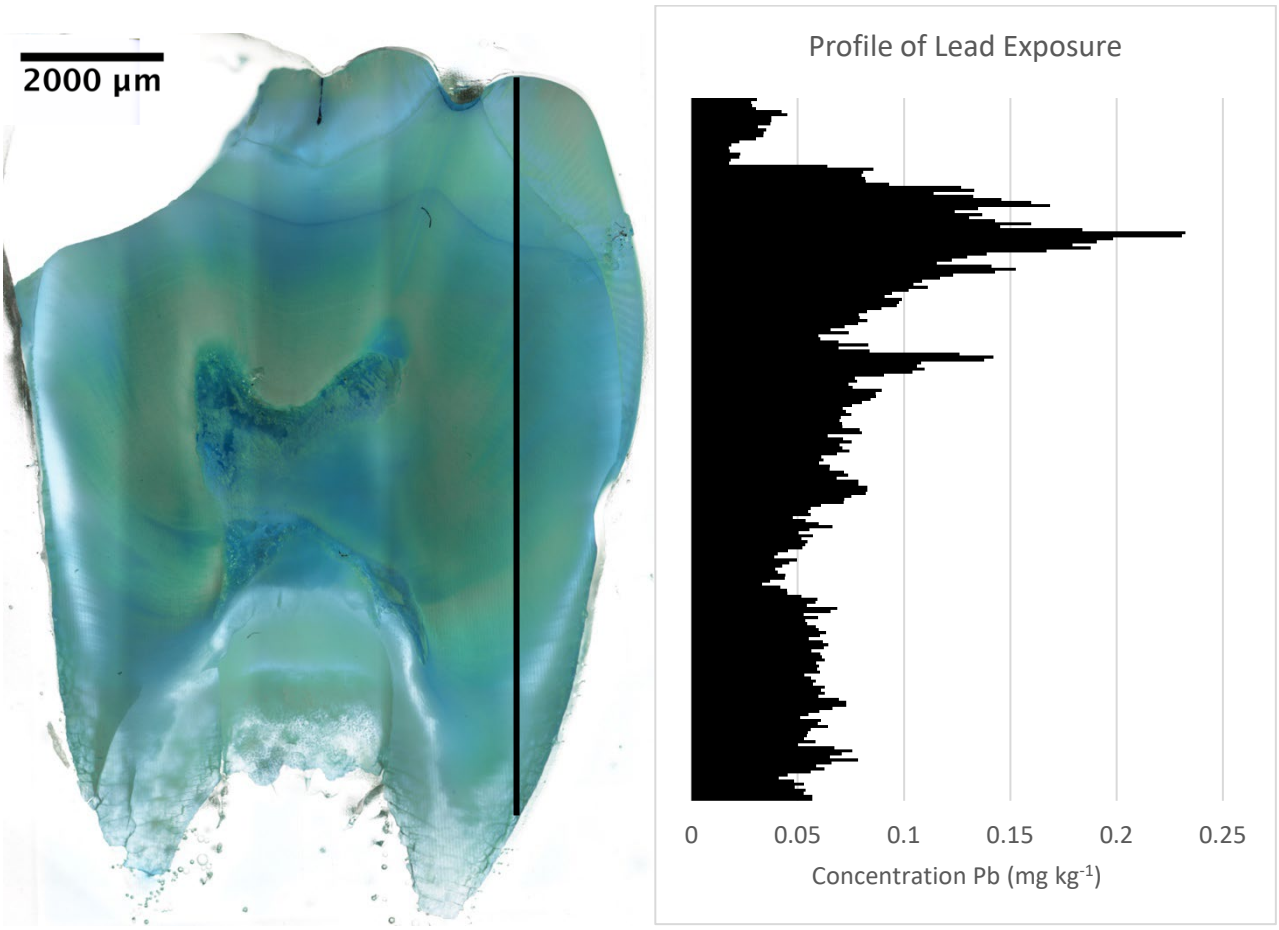

Figure 3. Optical micrograph of the Sri Lankan molar tooth taken and stitched together on the NIKON TI. Microscope. Black line indicates the transect of the tooth used to sample the profile of lead exposure.

Conclusions

Here, we prepared three artificial hydroxyapatite materials and assessed their suitability as external calibration standards for the LA-ICP-MS analysis of human teeth. The pelletised powder was the most suitable material, with facile fabrication, 8 homogeneously distributed elements, an equivalent ablation yield to teeth, and linear calibration curves with low LODs. Furthermore, it was compared against a method that use a one-point calibration against NIST glass and an internal standard factor to account for differences in ablation between the calibrant and the sample. Differences in concentration were observed compared to the new method described, along with ablation yields that indicated different physical characteristics that may impact the concentrations obtained. The two teeth analysed showed evidence of exposure to Pb and Cd, highlighting the potential of synthetic HA calibration materials for the analysis of bioindicators of heavy metal exposure.

Conflicts of interest

There are no conflicts of interest to declare.

References

1 M. Martinez, C. Bayne, D. Aiello, M. Julian, R. Gaume and M. Baudelet, Multi-elemental matrix-matched calcium hydroxyapatite reference materials for laser ablation: Evaluation on teeth by laser-induced breakdown spectroscopy, *Spectrochim. Acta Part B At. Spectrosc.*, 2019, **159**, 105650.

2 N. Miliszkiewicz, S. Walas and A. Tobiasz, Current approaches to calibration of LA-ICP-MS analysis, *J. Anal. At. Spectrom.*, 2015, **30**, 327–338.

3 M. Westerhausen, T. E. Lockwood, R. Gonzalez de Vega, A. Röhnelt, D. P. Bishop, N. Cole, P. Doble and D. Clases, Low background mould-prepared gelatine standards for reproducible quantification in elemental bio-imaging, *Analyst*, , DOI:10.1039/C9AN01580A.

4 T. S. Elsdon and B. M. Gillanders, Strontium incorporation into calcified structures: Separating the

effects of ambient water concentration and exposure time, *Mar. Ecol. Prog. Ser.*, 2005, **285**, 233–243.

5 B. R. Schöne, Z. Zhang, D. E. Jacob, D. P. Gillikin, T. Tütken, D. Garbe-Schönberg, T. Mcconnaughey and A. Soldati, Effect of organic matrices on the determination of the trace element chemistry (Mg, Sr, Mg/Ca, Sr/Ca) of aragonitic bivalve shells (Arctica islandica)—Comparison of ICP-OES and LA-ICP-MS data, *Geochem. J.*, 2010, **44**, 23–37.

6 A. M. Fowler, P. I. Macreadie, D. P. Bishop and D. J. Booth, Using otolith microchemistry and shape to assess the habitat value of oil structures for reef fish, *Mar. Environ. Res.*, 2015, **106**, 103–113.

7 G. M. Locosselli, K. Chacón-Madrid, M. A. Zezzi Arruda, E. Pereira de Camargo, T. C. Lopes Moreira, C. D. Saldiva de André, P. Afonso de André, J. M. Singer, P. H. Nascimento Saldiva and M. S. Buckeridge, Tree rings reveal the reduction of Cd, Cu, Ni and Pb pollution in the central region of São Paulo, Brazil, *Environ. Pollut.*, 2018, **242**, 320–328.

8 C. Figueroa-Romero, K. A. Mikhail, C. Gennings, P. Curtin, G. A. Bello, T. M. Botero, S. A. Goutman, E. L. Feldman, M. Arora and C. Austin, Early life metal dysregulation in amyotrophic lateral sclerosis, *Ann. Clin. Transl. Neurol.*, 2020, **7**, 872–882.

9 P. Budd, J. Montgomery, J. Evans and B. Barreiro, Human tooth enamel as a record of the comparative lead exposure of prehistoric and modern people, *Sci. Total Environ.*, 2000, **263**, 1–10.

10 D. Kang, D. Amarasiriwardena and A. H. Goodman, Application of laser ablation-inductively coupled plasma-mass spectrometry (LA-ICP-MS) to investigate trace metal spatial distributions in human tooth enamel and dentine growth layers and pulp, *Anal. Bioanal. Chem.*, 2004, **378**, 1608–1615.

11 B. Claus Henn, C. Austin, B. A. Coull, L. Schnaas, C. Gennings, M. K. Horton, M. Hernández-Ávila, H. Hu, M. M. Téllez-Rojo, R. O. Wright and M. Arora, Uncovering neurodevelopmental windows of susceptibility to manganese exposure using dentine microspatial analyses, *Environ. Res.*, 2018, **161**, 588–598.

12 C. N. Trueman and N. Tuross, in *Phosphates: Geochemical, Geobiological and Materials Importance*, De Gruyter Mouton, 2019, vol. 48, pp. 489–522.

13 D. Hare, C. Austin, P. Doble and M. Arora, Elemental bio-imaging of trace elements in teeth using laser ablation-inductively coupled plasma-mass spectrometry., *J. Dent.*, 2011, **39**, 397–403.

14 M. Arora, B. J. Kennedy, S. Elhlou, N. J. Pearson, D. M. Walker, P. Bayl and S. W. Y. Chan, Spatial distribution of lead in human primary teeth as a biomarker of pre- and neonatal lead exposure, *Sci. Total Environ.*, 2006, **371**, 55–62.

15 M. L. Praamsma and P. J. Parsons, Calibration strategies for quantifying the Mn content of tooth and bone samples by LA-ICP-MS, *Accredit. Qual. Assur.*, 2016, **21**, 385–393.

16 N. G. Miles, G. L. Butler, S. L. Diamond, D. P. Bishop, D. E. van der Meulen, I. Reinfelds and C. T. Walsh, Combining otolith chemistry and telemetry to assess diadromous migration in pinkeye mullet, Trachystoma petardi (Actinopterygii, Mugiliformes), *Hydrobiologia*, 2018, **808**, 265–281.

17 H. P. Longerich, S. E. Jackson and D. Günther, Inter-laboratory note. Laser ablation inductively coupled plasma mass spectrometric transient signal data acquisition and analyte concentration calculation, *J. Anal. At. Spectrom.*, 2004, **11**, 899–904.

18 S. E. Jackson, in *Laser Ablation-ICP-MS in the Earth Sciences: Current Practices and Outstanding Issues*, ed. P. Sylvester, Mineralogical Association of Canada, 2008, pp. 169–188.

19 A. Ugarte, N. Unceta, C. Pécheyran, M. A. Goicolea and R. J. Barrio, Development of matrix-matching hydroxyapatite calibration standards for quantitative multi-element LA-ICP-MS analysis: Application to the dorsal spine of fish, *J. Anal. At. Spectrom.*, 2011, **26**, 1421–1427.

20 W. Boer, S. Nordstad, M. Weber, R. Mertz-Kraus, B. Hönisch, J. Bijma, M. Raitzsch, D. Wilhelms-Dick, G. L. Foster, H. Goring-Harford, D. Nürnberg, F. Hauff, H. Kuhnert, F. Lugli, H. Spero, M. Rosner, P. van Gaever, L. J. de Nooijer and G. Reichart, A New Calcium Carbonate Nano-Particulate Pressed Powder Pellet (NFHS-2-NP) for LA-ICP-OES, LA-(MC)-ICP-MS and µXRF, *Geostand. Geoanalytical Res.*, , DOI:10.1111/ggr.12425.

21 A. Turyanskaya, S. Smetaczek, V. Pichler, M. Rauwolf, L. Perneczky, A. Roschger, P. Roschger,

P. Wobrauschek, A. Limbeck and C. Streli, Correlation of μXRF and LA-ICP-MS in the analysis of a human bone-cartilage sample, *J. Anal. At. Spectrom.*, 2021, **36**, 1512–1523.

22 S. Gruhl, F. Witte, J. Vogt and C. Vogt, Determination of concentration gradients in bone tissue generated by a biologically degradable magnesium implant, *J. Anal. At. Spectrom.*, 2009, **24**, 181–188.

23 A. Ugarte, N. Unceta, C. Pécheyran, M. A. Goicolea and R. J. Barrio, Development of matrix-matching hydroxyapatite calibration standards for quantitative multi-element LA-ICP-MS analysis: application to the dorsal spine of fish, *J. Anal. At. Spectrom.*, 2011, **26**, 1421.

24 J. Draxler, A. Zitek, M. Meischel, S. E. Stranzl-Tschegg, B. Mingler, E. Martinelli, A. M. Weinberg and T. Prohaska, Regionalized quantitative LA-ICP-MS imaging of the biodegradation of magnesium alloys in bone tissue, *J. Anal. At. Spectrom.*, 2015, **30**, 2459–2468.

25 T. Bazin, A. Magnaudeix, R. Mayet, P. Carles, I. Julien, A. Demourgues, M. Gaudon and E. Champion, Sintering and biocompatibility of copper-doped hydroxyapatite bioceramics, *Ceram. Int.*, 2021, **47**, 13644–13654.

26 K. Ulens, L. Moens, R. Dams, S. Van Winckel and L. Vandevelde, Study of element distributions in weathered marble crusts using laser ablation inductively coupled plasma mass spectrometry, *J. Anal. At. Spectrom.*, 1994, **9**, 1243.

27 J. Lear, D. Hare, P. Adlard, D. Finkelstein and P. Doble, Improving acquisition times of elemental bio-imaging for quadrupole-based LA-ICP-MS, *J. Anal. At. Spectrom.*, 2012, **27**, 159–164.

28 T. E. Lockwood, M. T. Westerhausen and P. A. Doble, Pew2: Open-Source Imaging Software for Laser Ablation-Inductively Coupled Plasma-Mass Spectrometry, *Anal. Chem.*, 2021, **93**, 10418–10423.

29 M. E. Shaheen, J. E. Gagnon and B. J. Fryer, Evaluation of ablation efficiency and surface morphology of human teeth upon irradiation with femtosecond laser pulses, *Laser Phys.*, , DOI:10.1088/1054-660X/24/11/116001.

30 J. H. Yoo, S. H. Jeong, R. Greif and R. E. Russo, Explosive change in crater properties during high

power nanosecond laser ablation of silicon, *J. Appl. Phys.*, 2000, **88**, 1638.

31 S. Bruckner, G. Lusvardi, L. Menabue and M. Saladini, Effect of Cu2+ ion on the structural stability of synthetic hydroxyapatite, *J. Mater. Chem.*, 1993, **3**, 715–719.

32 A. Nzihou, B. Adhikari and R. Pfeffer, Effect of metal chlorides on the sintering and densification of hydroxyapatite adsorbent, *Ind. Eng. Chem. Res.*, 2005, **44**, 1787–1794.

33 A. Cucina, J. Dudgeon and H. Neff, Methodological strategy for the analysis of human dental enamel by LA-ICP-MS, *J. Archaeol. Sci.*, 2007, **34**, 1884–1888.

34 C. Austin, T. M. Smith, A. Bradman, K. Hinde, R. Joannes-Boyau, D. Bishop, D. J. Hare, P. Doble, B. Eskenazi and M. Arora, Barium distributions in teeth reveal early-life dietary transitions in primates, *Nature*, 2013, **498**, 216–219.

35 M. Arora, D. Hare, C. Austin, D. R. Smith and P. Doble, Spatial distribution of manganese in enamel and coronal dentine of human primary teeth., *Sci. Total Environ.*, 2011, **409**, 1315–9.

36 W. Müller, A. Nava, D. Evans, P. F. Rossi, K. W. Alt and L. Bondioli, Enamel mineralization and compositional time-resolution in human teeth evaluated via histologically-defined LA-ICPMS profiles, *Geochim. Cosmochim. Acta*, 2019, **255**, 105–126.

37 R. Joannes-Boyau, J. W. Adams, C. Austin, M. Arora, I. Moffat, A. I. R. Herries, M. P. Tonge, S. Benazzi, A. R. Evans, O. Kullmer, S. Wroe, A. Dosseto and L. Fiorenza, Elemental signatures of Australopithecus africanus teeth reveal seasonal dietary stress, *Nature*, 2019, **572**, 112–115.

38 C. Stadlbauer, C. Reiter, B. Patzak, G. Stingeder and T. Prohaska, History of individuals of the 18th/19th centuries stored in bones, teeth, and hair analyzed by LA-ICP-MS-a step in attempts to confirm the authenticity of Mozart's skull, *Anal. Bioanal. Chem.*, 2007, **388**, 593–602.

39 M. Martinez, C. Bayne, D. Aiello, M. Julian, R. Gaume and M. Baudelet, Multi-elemental matrix-matched calcium hydroxyapatite reference materials for laser ablation: Evaluation on teeth by laser-induced breakdown spectroscopy, *Spectrochim. Acta - Part B At. Spectrosc.*, 2019, **159**, 105650.

40 J. L. Stroud, P. H. Buschang and P. W. Goaz, Sexual dimorphism in mesiodistal dentin and enamel

thickness., *Dentomaxillofacial Radiol.*, 1994, **23**, 169–171.

41 F. E. Grine, Enamel thickness of deciduous and permanent molars in modernHomo sapiens, *Am. J. Phys. Anthropol.*, 2005, **126**, 14–31.

42 C. Bellucci and N. Perrini, A study on the thickness of radicular dentine and cementum in anterior and premolar teeth, *Int. Endod. J.*, 2002, **35**, 594–606.

43 E.-L. LAKOMAA and I. RYTÖMAA, Mineral composition of enamel and dentin of primary and permanent teeth in Finland, *Eur. J. Oral Sci.*, 1977, **85**, 89–95.

44 R. de F. Z. Lizarelli, L. T. Moriyama, J. R. P. Jorge and V. S. Bagnato, Comparative ablation rate from a Er: YAG laser on enamel and dentin of primary and permanent teeth, *Laser Phys.*, 2006, **16**, 849–858.

45 W. D. Seka, J. D. B. Featherstone, D. Fried, S. R. Visuri and J. T. Walsh, in *Lasers in Dentistry II*, eds. H. A. Wigdor, J. D. B. Featherstone, J. M. White and J. Neev, 1996, vol. 2672, p. 144.

46 M. Arora, C. Austin, B. Sarrafpour, M. Hernandez-Avila, H. Hu, R. Wright and M. Tellez-Rojo, Determining Prenatal, Early Childhood and Cumulative Long-Term Lead Exposure Using Micro-Spatial Deciduous Dentine Levels: e97805, *PLoS One*, , DOI:10.1371/journal.pone.0097805.

47 A. A. Fouad and I. Jresat, Protective effect of telmisartan against cadmium-induced nephrotoxicity in mice, *Life Sci.*, 2011, **89**, 29–35.

48 A. L. Wani, A. Ara and J. A. Usmani, Lead toxicity: A review, *Interdiscip. Toxicol.*, 2015, **8**, 55–64.

49 A. F. Marques, J. P. Marques, C. Casaca and M. L. Carvalho, X-ray microprobe synchroton radiation X-ray fluorescence application on human teeth of renal insufficiency patients, *Spectrochim. Acta Part B At. Spectrosc.*, 2004, **59**, 1675–1680.

50 A. R. Sitarik, M. Arora, C. Austin, L. F. Bielak, S. Eggers, C. C. Johnson, S. V Lynch, S. Kyun, K. H. Wu, G. J. M. Yong and A. E. Cassidy-bushrow, Fetal and early postnatal lead exposure measured in teeth associates with infant gut microbiota, *Environ. Int.*, 2020, **144**, 106062.